


## Mean-Field Theory of Yielding under Oscillatory Shear

Jack T. Parley <sup>\*</sup>

*Institut für Theoretische Physik, University of Göttingen, Friedrich-Hund-Platz 1, 37077 Göttingen, Germany*

Srikanth Sastry 

*Jawaharlal Nehru Centre for Advanced Scientific Research, Jakkur Campus, 560064 Bengaluru, India*

Peter Sollich 

*Institut für Theoretische Physik, University of Göttingen, Friedrich-Hund-Platz 1, 37077 Göttingen, Germany  
and Department of Mathematics, King's College London, London WC2R 2LS, United Kingdom*



(Received 25 January 2022; accepted 13 April 2022; published 12 May 2022)

We study a mean field elastoplastic model, embedded within a disordered landscape of local yield barriers, to shed light on the behavior of athermal amorphous solids subject to oscillatory shear. We show that the model presents a genuine dynamical transition between an elastic and a yielded state, and qualitatively reproduces the dependence on the initial degree of annealing found in particle simulations. For initial conditions prepared below the analytically derived threshold energy, we observe a nontrivial, nonmonotonic approach to the yielded state. The timescale diverges as one approaches the yielding point from above, which we identify with the fatigue limit. We finally discuss the connections to brittle yielding under uniform shear.

DOI: [10.1103/PhysRevLett.128.198001](https://doi.org/10.1103/PhysRevLett.128.198001)

The behavior of amorphous solids (characterized by the lack of any regular structure) under deformations is of great practical importance, and has long been an active topic because the disorder inherent in these systems poses a significant challenge to their understanding [1–3]. These materials typically show yielding behavior: although they behave elastically at small deformation, plastic deformation eventually sets in, leading to a flowing state. Given the large variety of amorphous solids, ranging from hard metallic glasses to soft colloidal gels or emulsions, so-called elastoplastic models [3] aim for a unified description from a statistical physics point of view.

A key aspect of yielding under uniform shear, which has received much attention recently [4–10], concerns the dependence on the initial degree of annealing—quantified by potential energy—of the amorphous solid (or “glass” for short) before deformation starts. Typically, it is found that poorly annealed glasses yield in a smooth, ductile manner, with plastic deformation appearing gradually, while well annealed glasses may yield in a brittle manner, accompanied by a macroscopic stress drop. Under start-up of steady shear, although some features are still debated [9], there is strong evidence that, at least in the brittle case, and under quasistatic loading, yielding corresponds to a discontinuous nonequilibrium transition, which in finite-dimensional systems is accompanied by the sudden appearance of a unique system-spanning shear band [5–8].

Yielding under oscillatory shear has until recently received less attention, although it may in some respects

be a more informative protocol than the uniform case. One advantage is that one may directly probe the steady state after many cycles both below and above the yield point, whereas in the uniform case the states up to yielding are inherently transient. Furthermore, oscillatory strain allows one to relate macroscopic yielding directly to a sharp absorbing-to-diffusive transition in the nature of the microscopic trajectories [11–15] and to shear jamming [16–20].

Behavior under oscillatory shear also shows intriguing dependencies on the initial degree of annealing. Atomistic simulations of model glasses [21–23] reveal the appearance of a threshold initial energy. Samples prepared above this threshold show mechanical annealing up to a common strain amplitude, the yield point, where the energy achieves the threshold value irrespectively of the initial condition. On approaching the yield point in strain, the timescale to anneal to the threshold energy appears to diverge [11,13–15]. On the other hand, samples prepared below the threshold are insensitive to shear up to an initial condition-dependent critical strain *above the common yield point*, where they then yield abruptly.

Recent attempts to tackle this problem include energy landscape based [24,25] and 2D lattice elastoplastic models [26,27]. While the elastoplastic models [26,27] defy analytical progress as they implement the full spatial interaction kernel, the approach of Ref. [25] ignores interactions between elements, and indeed does not display a genuine yielding transition as the steady state after sufficiently many cycles is always elastic. An Ehrenfest-type model has also

been proposed along these lines [28]. This incorporates a simplified form of mechanical noise but does not explicitly represent oscillatory shear.

Here, we consider a model with a single element description that is similar to Refs. [25,26] in the way that it accounts for the disordered energy landscape, while including the elastic interactions in a mean field manner that allows for analytical progress. Importantly, we find a steady state yielding transition and are able to reproduce qualitatively all the main features of yielding under oscillatory shear described above.

*Disordered HL model.*—The Hébraud-Lequeux (HL) model for the rheology of amorphous solids [29] is a mean field mesoscopic elastoplastic model, which despite its many idealizations has had remarkable successes and been widely studied [30–36]. The material is conceptually divided into mesoscopic elements, large enough to carry a local elastic strain  $l$  and stress  $\sigma = kl$ ; these are related by an elastic modulus  $k$  that is considered to be uniform throughout the system for simplicity. In the elastoplastic approach, the dynamics of the elements is described as consisting of periods of elastic loading interrupted by plastic events that are accompanied by a local stress drop. In a mean field fashion, the effect of stress propagation from other yield events is considered as a mechanical noise [3,32], leading to a diffusive dynamics in the local strain  $l$  (or equivalently the stress).

In the original HL model [29], all elements have a common strain threshold related to the common yield energy  $E$  as  $l_c = \sqrt{2E/k}$ . However, due to the oversimplification of considering one single energy barrier throughout the system, this model is unable to capture the rich phenomenology under oscillatory shear found in particle simulations, for which it is essential to take into account the full energy landscape each mesoscopic element has access to.

An extension of the HL model to include this energy landscape, following previous approaches such as the soft glassy rheology model [37], was introduced in Ref. [32]. The essential ingredient is the disorder in the depth  $E$  of the energy minima relative to a common reference energy, characterized by a distribution  $\rho(E)$ . Each time an element yields, it occupies a new local minimum with a depth extracted from this distribution. The depth  $E$  of the current local energy minimum is thus promoted to a stochastic variable, and the system is described by a joint distribution  $P(E, l)$  evolving as

$$\partial_t P(E, l, t) = -\dot{\gamma} \partial_l P + D(t) k^{-2} \partial_l^2 P + Y(t) \rho(E) \delta(l) - \tau_{\text{pl}}^{-1} \theta(|l| - \sqrt{2E/k}) P \quad (1)$$

with

$$Y(t) = \frac{1}{\tau_{\text{pl}}} \int_0^\infty dE \int_{-\infty}^\infty dl P(E, l, t) \theta\left(|l| - \sqrt{\frac{2E}{k}}\right) \quad (2)$$

where  $\theta$  and  $\delta$  denote the Heaviside and delta functions, respectively, and  $\dot{\gamma}$  is the applied shear rate.  $\tau_{\text{pl}}^{-1}$ , the plastic rate, is the rate at which a plastic event occurs once an element is strained beyond its yield threshold. We fix energy and time units by setting  $k = 1$  and  $\tau_{\text{pl}} = 1$ . The quantity  $Y(t)$  in Eq. (2) is the *yield rate*, i.e., the fraction of elements that yield per unit time. The key feature of the model is the *closure relation* relating the yield rate to the diffusion constant  $D(t)$ . We adopt the simple proportionality  $D(t) = \alpha Y(t)$  [29]. The coupling constant  $\alpha$  effectively sets the strength of the interactions, and under certain assumptions can be directly related to the elastic stress propagator [32,38]. In the Supplemental Material [39] we check that a more general closure relation, which reflects the fact that yield events contribute differently to the noise depending on their local barrier, leaves the theory essentially unchanged, with only slight quantitative changes in the transient behavior.

After its introduction in Ref. [32], the approach described by Eqs. (1) and (2) has not been developed further as it is somewhat unwieldy to tackle analytically; in particular it has not been used to study oscillatory shear. Our first contribution will be to determine a dynamical transition in Eq. (1) under oscillatory shear, separating a frozen elastically deforming solid state from a yielded state.

*Transition line.*—We consider applying oscillatory shear  $\gamma(t) = \gamma_0 \sin(\omega t)$  in Eq. (1), with a fixed low frequency  $\omega \ll 1$  so that we are in the quasistatic regime. The two control parameters are thus the strain amplitude  $\gamma_0$  and the coupling constant  $\alpha$ . For convenience, we introduce the rescaled versions  $\tilde{\gamma}_0 = \gamma_0 / \sqrt{\langle E \rangle}$  and  $\tilde{\alpha} = \alpha / \langle E \rangle$ ,  $\langle E \rangle$  being the average over the disorder distribution  $\rho(E)$ . From Ref. [32], the physically relevant parameter regime of the disordered HL model is known to be  $\tilde{\alpha} < 1$ , where the system is jammed in the absence of shear. Within this jammed regime, we now calculate the transition line  $\tilde{\gamma}_0^*(\tilde{\alpha})$  above which there exists a yielded steady state.

We proceed as follows. At a fixed  $\tilde{\alpha}$ , suppose  $\tilde{\gamma}_0$  is large enough so that Eq. (1) has a yielded steady state. Rescaling time by the period  $T$  so that  $\tau = t/T = \omega t / (2\pi)$ ,  $\tau \in [0, 1]$ , this steady state is characterized by a nonzero period-averaged yield rate  $\bar{Y} = \int_0^1 Y(\tau) d\tau$ . As  $\tilde{\gamma}_0$  is decreased toward  $\tilde{\gamma}_0^*$ , we take  $\bar{Y}$  to vanish smoothly—an assumption we show to be self-consistent in the end—with the rescaled yield rate  $Y(\tau)/\bar{Y} = y(\tau)$  approaching a limiting form. In this limit, the key observation from the dynamical equations [Eqs. (1) and (2)] is that the local yielding events can be classified into two distinct groups.

Suppose an element yields at a time  $\tau' \in [0, 1]$  within the period, and is assigned a new energy depth  $E$ . Neglecting strain diffusion, its local strain will subsequently evolve as  $l(\tau) = \gamma(\tau) - \gamma(\tau')$ . If  $\gamma_0 + |\gamma(\tau')| < \sqrt{2E}$ , this element will therefore not be able to yield again in the next cycle; its strain will have to change diffusively (due to mechanical

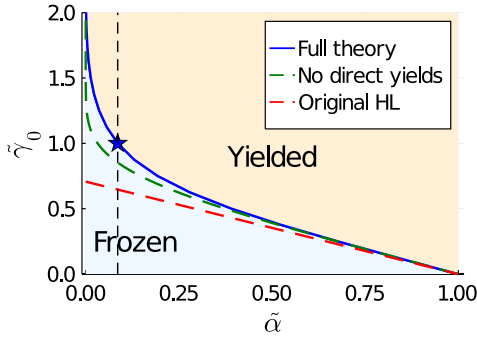


FIG. 1. Phase diagram of the model in the  $\tilde{\alpha} - \tilde{\gamma}_0$  plane for a Gaussian  $\rho(E)$ . Vertical dashed lines indicate the fixed coupling value  $\tilde{\alpha} = 0.086$ , where  $\tilde{\gamma}_0^* = 1$  (see star), chosen for studying the initial annealing dependence.

noise) during a large number of ensuing cycles until it comes close enough to the threshold  $\sqrt{2E}$  to be swept across it by the external shear. In the limit of vanishing strain diffusion, this will occur precisely at either the strain maximum or minimum within the cycle ( $\tau = 1/4$  or  $3/4$ ).

The second group of events is the *direct yields*. If  $\gamma_0 + |\gamma(\tau')| \geq \sqrt{2E}$ , the element will yield within the ensuing cycle. It will do so at a time  $\tau_y$  during the cycle that will depend on the previous yield time  $\tau'$  and the corresponding shear strain  $\gamma(\tau') = \gamma_0 \sin(2\pi\tau')$ , as well as on  $E$  and  $\gamma_0$ .

Overall, one can therefore separate the limiting yield rate into two contributions as  $y(\tau) = y^{(1)}(\tau) + y^{(2)}(\tau)$ , corresponding to indirect and direct yields respectively. Conservation of probability then implies the following pair of self-consistent equations:

$$\begin{aligned}
 y^{(1)}(\tau) &= \frac{1}{2} [\delta(\tau - 1/4) + \delta(\tau - 3/4)] \int_{\gamma_0^2/2}^{\infty} dE \rho(E) \\
 &\quad \times \int_0^1 d\tau' y(\tau') \theta(\sqrt{2E} - \gamma_0 - |\gamma_0 \sin(2\pi\tau')|) \\
 y^{(2)}(\tau) &= \int_0^{\infty} dE \rho(E) \\
 &\quad \times \int_0^1 d\tau' y(\tau') \delta\{\tau - \tau_y[\tau', \gamma_0 \sin(2\pi\tau'), \gamma_0, E]\} \quad (3)
 \end{aligned}$$

which can be solved numerically in an iterative way [39].

Once the limiting form of the yield rate  $y(\tau)$  is known, the full steady state distribution at the transition  $P^*(E, l)$  can be obtained straightforwardly by applying the diffusion propagator with absorbing boundary conditions at the local yield thresholds. The critical coupling  $\tilde{\alpha}^*(\tilde{\gamma}_0)$  is then found by imposing normalization of this distribution, and arises from the interplay between the disordered landscape and the timescale set by the mechanical noise. A key property of  $P^*(E, l)$  is that it is nonzero only for values  $(E, l)$  from

which all yields are indirect. The steady state probability of other elements vanishes as  $\bar{Y}/\omega$  at the transition, but they still contribute to the total yield rate as they have yield rates  $\sim \omega$ .

Figure 1 shows the transition line for the specific case of a Gaussian yield energy distribution  $\rho(E) \sim e^{-E^2/(2\sigma^2)}$ . This is the form for  $\rho(E)$  we will adopt in the rest of the work [40], to match the results of earlier numerical studies [41]. In Fig. 1 we also show the approximate solution obtained if one neglects direct yields; this is exact for  $\tilde{\alpha} \rightarrow 1$ . This approximation is useful to derive an exact bound [39] proving in general that in the presence of disorder the phase boundary lies above the original HL model: the inclusion of disorder (which entails deep traps where elements may get stuck) always tends to extend the size of the frozen region.

*Dependence on initial degree of annealing.*—Although we have proven that in the yielded region of Fig. 1 a fluid steady state *exists*, whether this ergodic state is reached depends crucially on the initial condition. We now study the master equation [Eq. (1)] numerically, while fixing  $\tilde{\alpha} = 0.086$  (where  $\tilde{\gamma}_0^* \approx 1$ , see star in Fig. 1), and setting the variance of the Gaussian to  $\sigma = 0.05$  as in Ref. [25]. Numerical solutions entail choosing a discrete set of energy levels  $\{E_i\}$ , and solving a partial differential equation in the strain variable for each [39]. As a proxy for different degrees of *thermal annealing* of the initial glass, we generate initial conditions of the form  $P(E, t = 0) \sim \rho(E)e^{\beta E}$ , introducing an inverse temperature  $\beta$ . Physically, increasing  $\beta$  can be interpreted as decreasing the density of weak zones in the system, here represented by the shallow energy levels. As regards the initial local strains, we consider them to be well relaxed (narrowly distributed) within each energy level, with standard deviation in strain  $l_c(E)/6$ .

In Fig. 2 we show the stroboscopic ( $\gamma = 0$ ) energy in the steady state after the application of many cycles of shear at

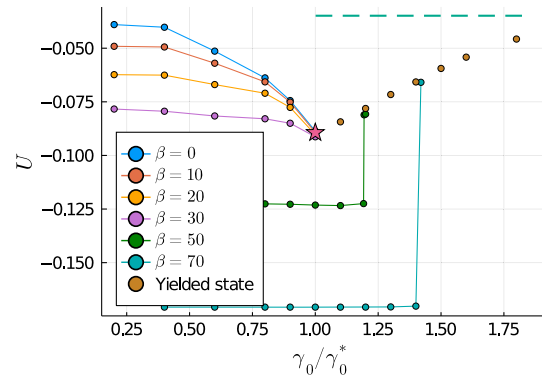


FIG. 2. Stroboscopic energy in the steady state after application of many cycles of shear with amplitude  $\gamma_0$ . Star indicates analytically calculated threshold energy  $U^*$ ; dashed line corresponds to the steady shear limit reached as  $\gamma_0 \rightarrow \infty$ , known from Ref. [32]. Steady state energy values for  $\gamma_0 = \gamma_0^*$  and  $0.9\gamma_0^*$  are obtained from a power-law extrapolation of the slow relaxation [39].

a given amplitude  $\gamma_0$ . On the solid side, this corresponds to a frozen state with  $\bar{Y} = 0$ ; on the yielded side, this is the ergodic state with  $\bar{Y} > 0$ . The total energy is measured within the model as  $U = \int dE \int dl (-E + l^2/2) P(E, l)$ , i.e., energy at the bottom of each minimum plus elastic energy, while the macroscopic stress (see below) is  $\Sigma = \int dE \int dl l P(E, l)$ . The main features found in MD simulations [21–23] are reproduced in Fig. 2. Within the precision and range of our numerics, yielding for poorly annealed samples appears as a cusp in  $U$  at the common yield point  $\gamma_0^*$ , while well-annealed samples are insensitive to shear up to a critical strain  $\gamma_c(\beta) > \gamma_0^*$ . The threshold energy (and corresponding  $\beta^*$ ) separating the two types of yielding simply arises as the lower limit of the ergodic state. The corresponding data for the macroscopic stress amplitude in the steady state [39] also qualitatively reproduce the behavior in Refs. [15,21,22], with a finite drop in steady state macroscopic stress appearing for samples prepared below the threshold.

We note that the MD studies of Refs. [15,22,42] report a small (essentially invisible on the scale of Fig. 2) jump in energy and macroscopic stress amplitude at  $\gamma_0^*$ . The origin of this effect, which appears to survive for large system sizes, is unclear. We expect that in our mean field model both energy and stress remain continuous on approaching from the solid side, and our numerics are consistent with this. From the fluid side, our theory predicts that  $\bar{Y}$  vanishes continuously, reminiscent of, e.g., the second order transition scenario of Ref. [43]. Closer inspection reveals that samples initialized above the threshold energy display critical behavior at  $\gamma_0^*$ , where the yield rate decays as  $\bar{Y}(t) \sim t^{-b}$ , with an  $\tilde{\alpha}$ -dependent exponent  $b \leq 1$ . This implies a diverging number of events for long time, allowing the system to lose memory of its initial condition. The critical power-law decay of  $\bar{Y}(t)$  also means that relaxation timescales must diverge on the approach from either side of the transition.

*Fatigue.*—Turning to samples with initial energy below the threshold energy, which yield at  $\gamma_c(\beta) > \gamma_0^*$ , we find very interesting transient behavior. As shown in Fig. 3 for  $\beta = 50$ , close to  $\gamma_c(\beta)$  the yield rate  $\bar{Y}$  displays strongly nonmonotonic behavior. Although in our mean field model the yielded state is reached smoothly, one generally finds that in finite dimensional systems, once the plastic activity starts to increase, an instability develops leading to shear banding or even material failure [44]. As a proxy for the time to failure (expressed in number of cycles,  $n_f$  [45]), we take the inflection point of  $\bar{Y}(t)$  as done in Ref. [31] for creep (where it is associated to banding [46]), as well as the point at which  $\bar{Y}$  reaches 75% of its steady state value, which allows us to analyze larger  $\gamma_0$  where an inflection is not present. We additionally consider the number of cycles at which the minimum of  $\bar{Y}$  is reached. We find (Fig. 3) that the number of cycles  $n_f$  decreases rapidly (consistent with

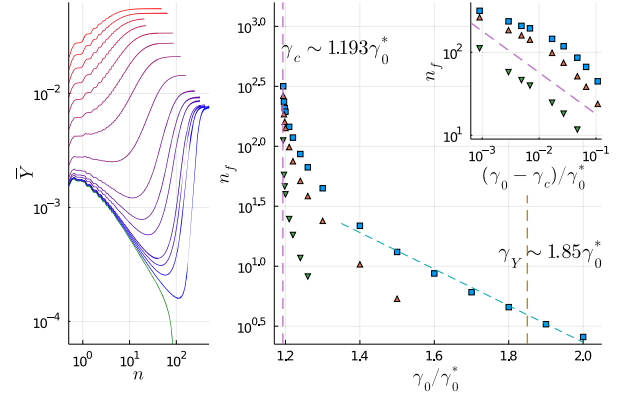


FIG. 3. *Fatigue* behavior for well-annealed sample ( $\beta = 50$ ). Left: nonmonotonic behavior of period-averaged yield rate  $\bar{Y}$  against number of cycles. Strain amplitudes  $\gamma_0$  range from  $1.194\gamma_0^*$  (blue) to  $2\gamma_0^*$  (red) (see the Supplemental Material [39] for precise values); also shown is  $1.192\gamma_0^*$  (green), below the fatigue limit. Right: for the same strain amplitudes, three measures of the fluidization time as described in the text, 75% of final yield rate (squares), inflection point (up-triangles), and cycles to reach the minimum (down-triangles). Inset: divergence of timescales above  $\gamma_c(\beta)$ , consistent with an inverse square root (dashed line) for the minimum.

an exponential) toward unity as  $\gamma_0$  is increased toward  $\gamma_Y$ , the yield point determined for  $\beta = 50$  under start-up of steady shear [39]. This is very reminiscent of *fatigue failure* [47–51] found, e.g., in metallic glasses. Close to  $\gamma_c(\beta)$ , the timescale associated to the minimum shows a clear power-law divergence, consistent with an inverse square root. The similarity of this mean field fatigue behavior with creep flow suggests the intriguing possibility that this divergence may be understood from a Landau-type scaling argument as recently proposed in Ref. [52] for creep.

A closer look at the dynamics of the mean field model near  $\gamma_c$  reveals that, during the initial cycles, the plastic activity is dominated by direct yielding of rare shallow elements [39], which we recall may be thought of as weak zones in the material. At intermediate times, the energy distribution  $P(E)$  then almost settles down to a frozen fixed point. However, eventually the accumulated strain diffusion is enough to trigger yield events across the entire energy spectrum (including deep levels where the bulk of the population lies), driving the system away toward the yielded steady state.

*Concluding remarks.*—In this Letter, we have presented a mean field mesoscopic elastoplastic approach to study yielding behavior under oscillatory shear. Our first contribution was to demonstrate the existence of a dynamical yielding transition and to characterize it analytically. Secondly, despite its relative simplicity, we have shown that the model reproduces the key phenomena related to initial annealing dependence found in MD studies [11,21,22]. Thirdly, we showed that the dynamics of well-annealed samples exhibits characteristics of fatigue



failure so that the model also contributes to the understanding of this phenomenon.

We comment finally on the contrast to brittle yielding under uniform shear, and the relative importance of shear banding. There are important differences between the two shear protocols, and these are also reflected in the mean field model. On the one hand, under oscillatory shear, both the existence of a sharp yield point and the initial annealing dependence (Fig. 2), which we recall concern *steady state* quantities, are largely unaffected by the shear rate  $\dot{\gamma}_0$  (equivalent to frequency via  $\dot{\gamma}_0 = \gamma_0 \omega$ ), and are independent of the presence of banding. This was found in MD studies [21] and is also supported here, where numerical results with finite frequency ( $\omega = 0.1$ ) largely agree with the  $\omega \rightarrow 0$  theory. Under uniform shear, on the other hand, brittle yielding can only strictly be defined for  $\dot{\gamma} \rightarrow 0$ , where a macroscopic stress drop is caused by the formation of a system-spanning shear band [8]. Indeed, under uniform shear, the disordered HL model shows no sign of brittle yielding even in the  $\dot{\gamma} \rightarrow 0$  limit, reflecting the absence of banding in mean field [53]. Regarding the *transient* dynamics under oscillatory shear, we expect the mean field model to become more accurate away from the quasistatic limit, as should the approximation of Gaussian mechanical noise [55].

As avenues of future research, one could improve upon the diffusive approximation and study the model with power-law mechanical noise [56,57]. It would also be interesting to include thermal activation over barriers (as in soft glassy rheology [28,37]) within the elastoplastic model, following Refs. [58,59]. Fascinating questions arise, starting with the phase diagram: would the existence of activation always lead to a yielded state? How will temperature influence the fatigue behavior?

The authors thank Suzanne Fielding, James Cochran, and Muhittin Mungan for helpful discussions. S. S. acknowledges support through the JC Bose Fellowship (JBR/2020/000015) SERB, DST (India).

---

\*To whom all correspondence should be addressed.  
jack.parley@uni-goettingen.de

- [1] D. Bonn, M. M. Denn, L. Berthier, T. Divoux, and S. Manneville, Yield stress materials in soft condensed matter, *Rev. Mod. Phys.* **89**, 035005 (2017).
- [2] L. Berthier and G. Biroli, Theoretical perspective on the glass transition and amorphous materials, *Rev. Mod. Phys.* **83**, 587 (2011).
- [3] A. Nicolas, E. E. Ferrero, K. Martens, and J.-L. Barrat, Deformation and flow of amorphous solids: Insights from elastoplastic models, *Rev. Mod. Phys.* **90**, 045006 (2018).
- [4] Y. Shi and M. L. Falk, Strain Localization and Percolation of Stable Structure in Amorphous Solids, *Phys. Rev. Lett.* **95**, 095502 (2005).
- [5] M. Ozawa, L. Berthier, G. Biroli, A. Rosso, and G. Tarjus, A random critical point separates brittle and ductile yielding transitions in amorphous materials, *Proc. Natl. Acad. Sci. U.S.A.* **115**, 6656 (2018).
- [6] M. Ozawa, L. Berthier, G. Biroli, and G. Tarjus, Rare events and disorder control the brittle yielding of amorphous solids, [arXiv:2102.05846](https://arxiv.org/abs/2102.05846).
- [7] M. Ozawa, L. Berthier, G. Biroli, and G. Tarjus, Role of fluctuations in the yielding transition of two-dimensional glasses, *Phys. Rev. Research* **2**, 023203 (2020).
- [8] M. Singh, M. Ozawa, and L. Berthier, Brittle yielding of amorphous solids at finite shear rates, *Phys. Rev. Mater.* **4**, 025603 (2020).
- [9] H. J. Barlow, J. O. Cochran, and S. M. Fielding, Ductile and Brittle Yielding in Thermal and Athermal Amorphous Materials, *Phys. Rev. Lett.* **125**, 168003 (2020).
- [10] H. Borja da Rocha and L. Truskinovsky, Rigidity-Controlled Crossover: From Spinodal to Critical Failure, *Phys. Rev. Lett.* **124**, 015501 (2020).
- [11] D. Fiocco, G. Foffi, and S. Sastry, Oscillatory athermal quasistatic deformation of a model glass, *Phys. Rev. E* **88**, 020301(R) (2013).
- [12] N. V. Priezjev, Heterogeneous relaxation dynamics in amorphous materials under cyclic loading, *Phys. Rev. E* **87**, 052302 (2013).
- [13] I. Regev, T. Lookman, and C. Reichhardt, Onset of irreversibility and chaos in amorphous solids under periodic shear, *Phys. Rev. E* **88**, 062401 (2013).
- [14] T. Kawasaki and L. Berthier, Macroscopic yielding in jammed solids is accompanied by a nonequilibrium first-order transition in particle trajectories, *Phys. Rev. E* **94**, 022615 (2016).
- [15] P. Leishangthem, A. D. S. Parmar, and S. Sastry, The yielding transition in amorphous solids under oscillatory shear deformation, *Nat. Commun.* **8**, 14653 (2017).
- [16] D. J. Pine, J. P. Gollub, J. F. Brady, and A. M. Leshansky, Chaos and threshold for irreversibility in sheared suspensions, *Nature (London)* **438**, 997 (2005).
- [17] L. Corté, P. M. Chaikin, J. P. Gollub, and D. J. Pine, Random organization in periodically driven systems, *Nat. Phys.* **4**, 420 (2008).
- [18] K. Nagasawa, K. Miyazaki, and T. Kawasaki, Classification of the reversible-irreversible transitions in particle trajectories across the jamming transition point, *Soft Matter* **15**, 7557 (2019).
- [19] P. Das, H. A. Vinutha, and S. Sastry, Unified phase diagram of reversible-irreversible, jamming, and yielding transitions in cyclically sheared soft-sphere packings, *Proc. Natl. Acad. Sci. U.S.A.* **117**, 10203 (2020).
- [20] V. Babu, D. Pan, Y. Jin, B. Chakraborty, and S. Sastry, Dilatancy, shear jamming, and a generalized jamming phase diagram of frictionless sphere packings, *Soft Matter* **17**, 3121 (2021).
- [21] W.-T. Yeh, M. Ozawa, K. Miyazaki, T. Kawasaki, and L. Berthier, Glass Stability Changes the Nature of Yielding under Oscillatory Shear, *Phys. Rev. Lett.* **124**, 225502 (2020).
- [22] H. Bhaumik, G. Foffi, and S. Sastry, The role of annealing in determining the yielding behavior of glasses under cyclic

- shear deformation, *Proc. Natl. Acad. Sci. U.S.A.* **118**, e2100227118 (2021).
- [23] H. Bhaumik, G. Foffi, and S. Sastry, Yielding transition of a two dimensional glass former under athermal cyclic shear deformation, *J. Chem. Phys.* **156**, 064502 (2022).
- [24] A. Szulc, O. Gat, and I. Regev, Forced deterministic dynamics on a random energy landscape: Implications for the physics of amorphous solids, *Phys. Rev. E* **101**, 052616 (2020).
- [25] S. Sastry, Models for the Yielding Behavior of Amorphous Solids, *Phys. Rev. Lett.* **126**, 255501 (2021).
- [26] C. Liu, E. E. Ferrero, E. A. Jagla, K. Martens, A. Rosso, and L. Talon, The fate of shear-oscillated amorphous solids, *J. Chem. Phys.* **156**, 104902 (2022).
- [27] K. Khirallah, B. Tyukodi, D. Vandembroucq, and C. E. Maloney, Yielding in an Integer Automaton Model for Amorphous Solids under Cyclic Shear, *Phys. Rev. Lett.* **126**, 218005 (2021).
- [28] M. Mungan and S. Sastry, Metastability as a Mechanism for Yielding in Amorphous Solids under Cyclic Shear, *Phys. Rev. Lett.* **127**, 248002 (2021).
- [29] P. Hébraud and F. Lequeux, Mode-Coupling Theory for the Pasty Rheology of Soft Glassy Materials, *Phys. Rev. Lett.* **81**, 2934 (1998).
- [30] E. Agoritsas and K. Martens, Non-trivial rheological exponents in sheared yield stress fluids, *Soft Matter* **13**, 4653 (2017).
- [31] C. Liu, K. Martens, and J.-L. Barrat, Mean-Field Scenario for the Athermal Creep Dynamics of Yield-Stress Fluids, *Phys. Rev. Lett.* **120**, 028004 (2018).
- [32] E. Agoritsas, E. Bertin, K. Martens, and J.-L. Barrat, On the relevance of disorder in athermal amorphous materials under shear, *Eur. Phys. J. E* **38**, 71 (2015).
- [33] F. Puosi, J. Olivier, and K. Martens, Probing relevant ingredients in mean-field approaches for the athermal rheology of yield stress materials, *Soft Matter* **11**, 7639 (2015).
- [34] J.-P. Bouchaud, S. Gualdi, M. Tarzia, and F. Zamponi, Spontaneous instabilities and stick-slip motion in a generalized Hébraud-Lequeux model, *Soft Matter* **12**, 1230 (2016).
- [35] T. Ekeh, E. Fodor, S. M. Fielding, and M. E. Cates, Power fluctuations in sheared amorphous materials: A minimal model, [arXiv:2106.12962](https://arxiv.org/abs/2106.12962).
- [36] P. Sollich, J. Olivier, and D. Bresch, Aging and linear response in the Hébraud-Lequeux model for amorphous rheology, *J. Phys. A* **50**, 165002 (2017).
- [37] P. Sollich, F. Lequeux, P. Hébraud, and M. E. Cates, Rheology of Soft Glassy Materials, *Phys. Rev. Lett.* **78**, 2020 (1997).
- [38] L. Bocquet, A. Colin, and A. Ajdari, Kinetic Theory of Plastic Flow in Soft Glassy Materials, *Phys. Rev. Lett.* **103**, 036001 (2009).
- [39] See Supplemental Material at <http://link.aps.org/supplemental/10.1103/PhysRevLett.128.198001> for details on analytical derivations and numerical solutions.
- [40] In the Supplement Material [39] we show that an exponential  $\rho(E)$  does not qualitatively change the form of the transition line, and argue more generally that our main results are qualitatively robust to the precise form of  $\rho(E)$ .
- [41] S. Sastry, The relationship between fragility, configurational entropy and the potential energy landscape of glass-forming liquids, *Nature (London)* **409**, 164 (2001).
- [42] A. D. S. Parmar, S. Kumar, and S. Sastry, Strain Localization Above the Yielding Point in Cyclically Deformed Glasses, *Phys. Rev. X* **9**, 021018 (2019).
- [43] C. Ness and M. E. Cates, Absorbing-State Transitions in Granular Materials Close to Jamming, *Phys. Rev. Lett.* **124**, 088004 (2020).
- [44] S. M. Fielding, Triggers and signatures of shear banding in steady and time-dependent flows, *J. Rheol.* **60**, 821 (2016).
- [45] For the number of cycles we simply take the time divided by the period, so that it takes continuous values in Fig. 3.
- [46] T. Divoux, C. Barentin, and S. Manneville, From stress-induced fluidization processes to Herschel-Bulkley behaviour in simple yield stress fluids, *Soft Matter* **7**, 8409 (2011).
- [47] H. A. Carmona, F. Kun, J. S. Andrade, and H. J. Herrmann, Computer simulation of fatigue under diametrical compression, *Phys. Rev. E* **75**, 046115 (2007).
- [48] S. Pradhan, A. Hansen, and B. K. Chakrabarti, Failure processes in elastic fiber bundles, *Rev. Mod. Phys.* **82**, 499 (2010).
- [49] B. P. Bhowmik, H. G. E. Hentschel, and I. Procaccia, Fatigue and collapse of cyclically bent strip of amorphous solid, [arXiv:2103.03040](https://arxiv.org/abs/2103.03040).
- [50] F. Kun, M. H. Costa, R. N. C. Filho, J. S. Andrade, J. B. Soares, S. Zapperi, and H. J. Herrmann, Fatigue failure of disordered materials, *J. Stat. Mech.* (2007) P02003.
- [51] Z. D. Sha, S. X. Qu, Z. S. Liu, T. J. Wang, and H. Gao, Cyclic deformation in metallic glasses, *Nano Lett.* **15**, 7010 (2015).
- [52] M. Popović, T. W. J. de Geus, W. Ji, A. Rosso, and M. Wyart, Scaling description of creep flow in amorphous solids, [arXiv:2111.04061](https://arxiv.org/abs/2111.04061).
- [53] In the Supplement Material [39] we provide more discussion and contrast this to the mean field results of [5,54].
- [54] M. Popović, T. W. J. de Geus, and M. Wyart, Elastoplastic description of sudden failure in athermal amorphous materials during quasistatic loading, *Phys. Rev. E* **98**, 040901(R) (2018).
- [55] C. Liu, E. E. Ferrero, F. Puosi, J.-L. Barrat, and K. Martens, Driving Rate Dependence of Avalanche Statistics and Shapes at the Yielding Transition, *Phys. Rev. Lett.* **116**, 065501 (2016).
- [56] J. T. Parley, S. M. Fielding, and P. Sollich, Aging in a mean field elastoplastic model of amorphous solids, *Phys. Fluids* **32**, 127104 (2020).
- [57] J. Lin and M. Wyart, Mean-Field Description of Plastic Flow in Amorphous Solids, *Phys. Rev. X* **6**, 011005 (2016).
- [58] M. Popović, T. W. J. de Geus, W. Ji, and M. Wyart, Thermally activated flow in models of amorphous solids, *Phys. Rev. E* **104**, 025010 (2021).
- [59] E. E. Ferrero, A. B. Kolton, and E. A. Jagla, Yielding of amorphous solids at finite temperatures, *Phys. Rev. Mater.* **5**, 115602 (2021).